

## **Optical Studies of ZnS Nanocrystalline Thin Films Deposited by Thermal Evaporation Technique.**

A.Elfalaky\*, H.A.Hashem and Amany Hamdy  
*Physics Department, Faculty of Science, Zagazig University, Zagazig Egypt.*

---

### **Abstract:**

*A thin film of Zinc Sulfide (ZnS) nanoparticles was deposited on quartz substrate under vacuum using thermal evaporation technique at room temperature. The X-ray diffraction pattern was used to analyze the surface morphology and find the particle size.*

*The optical transmission and reflection spectra have been measured in the wavelength range 190 – 2400 nm. The optical constants were estimated at different photon energy in the range between 0.5 and 3.5 eV. Besides, the absorption coefficient, type of optical transition, type of optical gap and energy gap of ZnS thin film were revealed.*

*The photoluminescence spectrum study of the as prepared ZnS thin film was found to exhibit a broad peak, with different emission peaks, which may be attributed to different defect levels.*

**Keywords:** nanoparticles, ZnS, Thin films, Optical and Photoluminescence.

---

Date of Submission: 02-05-2020

Date of Acceptance: 16-05-2020

---

### **I. Introduction:**

One of the most attracted semiconductor materials (among the II-VI compound materials) is Zinc sulfide (ZnS) which has a wide energy bandgap (3.6 eV) and direct optical transition at room temperature [1-3].

Zinc sulfide can be formed in two different crystal structures with the same bandgap energy (zinc blende and wurtzite). ZnS has been used in many application aspects such as field emission display, the cathode ray tube and the scintillator as one of the most frequently used phosphors [4, 5]. Besides, thin films of ZnS can be used as an active emitting material in such a device, termed the hot electron cold cathode [6]. For all that mentioned, the potential applications such as optoelectronics, solar cells, and ultraviolet light-emitting diodes, sensors, flat panel displays, antimicrobial activities, electroluminescent and photocatalytic are applications of ZnS thin film [7-9].

Many laboratory techniques have been used to deposit ZnS as a thin film like thermal evaporation, electrochemical deposition, spray pyrolysis, sputtering [10], Molecular beam epitaxy, RF reactive sputtering, Chemical bath deposition, ultrasonic spray, . . . etc. Among these techniques, the most interesting technique is the thermal evaporation technique because it has the advantages depend on the high stability [11], high deposition rate, high reproducibility, large-area deposition, and non-expensive. The thermal evaporation technique has helpful economical and provides evaporation of material by a constant rate of deposition.

The aim of this research is to illustrate the preparation of ZnS monocrySTALLINE thin films using the thermal evaporation method. Study the optical properties of the monocrySTALLINE material. To investigate the crystal structure and morphology of the prepared ZnS compound.

### **II. Experimental:**

#### **Chemicals:**

For the preparation of stoichiometric semiconducting ZnS thin films, the material used as a source is a nanoparticles powder of ZnS nanocrystal prepared in our lab using co-precipitation technique.

#### **Substrate cleaning:**

The important role of having high quality thin film by deposition is the substrate cleaning. The substrates were washed by hot distilled water and soap several times. By using the Branson-120 device, the substrates were exposed to ultrasonic waves for 15 minutes in a solution of distilled water and ethyl alcohol. Finally, the substrates were washed with distilled water and ethyl alcohol then, put in dry oven.

#### **Preparation of ZnS thin films:**

Particles of ZnS nanocrystals were prepared, before the deposition using the co-precipitation technique using the above chemicals.

The ZnS thin films of 630 nm thickness have been deposited on cleaned glass substrates at room temperature by the thermal evaporation technique. The film was fabricated under a vacuum of  $(5 \times 10^{-5}$  Torr). The nanoparticles of zinc sulfide are used as the source material. The stoichiometric starting source materials (ZnS) were loaded in a molybdenum boat and evaporated in a vacuum ( $5 \times 10^{-5}$  Torr) in the chamber system equipped with a nitrogen liquid trap.

At a distance of 140 mm, the source materials were kept far from the substrate holder in a vacuum chamber. During the deposition processes, the substrate was placed normal to the line of sight from the evaporation surface at different polar angles to obtain a uniform deposition.

#### **Characterization of thin films;**

##### **Structural characterization:**

The X-ray diffraction (XRD) pattern of the deposited thin film have been recorded by XRD, (Philips X' pert MPD, Panalytical, Netherlands) Nickel-filtered copper radiation with  $\lambda = 1.540 \text{ \AA}$ . The crystallite size,  $D$ , and dislocation density of deposited thin film were calculated by using Debye-Scherrer's formula [12].

$$D = \frac{0.94\lambda}{\beta \cos \theta} \quad (1)$$

$$\delta = \frac{1}{D^2} \quad (2)$$

where  $\lambda$  is wavelength of radiation used,  $\theta$  is diffraction angle of the concern diffraction peak,  $\beta$  is the full width at half maximum (FWHM) of the diffraction peak corresponding to a particular crystal plane and  $\delta$  is the dislocation density.

##### **Optical characterization:**

The optical transmission, reflection spectra were recorded by the spectral distribution of transmittance and reflectance of the film was measured using V-670 UV-VIS-NIR Spectrophotometer. The wavelength range was (190 – 2500 nm) at room temperature for the optical characterization of thin film that was deposited on a quartz substrate. The absorption coefficient ( $\alpha$ ) was calculated for the deposited thin film in the region of strong absorption using the relation.

$$\alpha = \frac{1}{d} \ln \left[ \frac{(1-R)^2 + \sqrt{(1-R)^4 + 4R^2T^2}}{2T} \right] \quad (3)$$

where  $\alpha$  is the absorption coefficient at particular wavelength,  $T$  is the transmittance at same wavelength, and  $d$  is the film thickness. The band gap of thin film has been calculated by using Tauc relation [13].

$$\alpha h\nu = A(h\nu - E_g)^n \quad (4)$$

where  $h\nu$  is photon energy,  $E_g$  is band gap,  $A$  is constant, and  $n = 2$  for direct band gap material.

##### **Photoluminescence characterization:**

Absorption and photoluminescence measurements have been carried out using a spectrophotometer and a spectrofluorometer (Jasco FP 6300) equipped with a xenon lamp.

### **III. Results and discussion:**

#### **Structural analysis of thin films:**

The X-ray diffraction pattern of the deposited ZnS thin film is shown in Fig. (1). The XRD measurement reveals that the peak broadening in the XRD pattern clearly indicates the formation of ZnS nanocrystal of small size. The cubic phase of the crystals has identified and confirmed the agreement of peak position with standard (ICDD) reference card **No. 04-004-3804**. The nanocrystals of ZnS have different planes (111), (220) and (311) [14]. The calculated average size using equation (1) was found to be 19.3 nm. The crystal structure gleaned from the x-rays investigated is cubic.

The pattern of ZnS nanocrystal as deposited thin film with thickness of 630 nm on a cleaned glass substrate obtained from X-ray diffraction is shown in Fig. (1), which confirms broad peaks indicating the formation of the film nanocrystallinity.

The standard (ICDD) reference card No. 04-004-3804 gives a good confirmation with the X-ray pattern peaks position indicating the main peak occurs at  $2\theta = 28.69^\circ$  with plane (111). The other peaks occur at  $2\theta = 48.70^\circ$  and  $50.09^\circ$  with different planes (220) and (311) respectively with preferential orientation along (111) plane and illustrate the cubic phase of nanocrystalline particles.

The experimental and standard d values of ZnS thin film are given in Table 1. The calculated average grain size was 19.3 nm and dislocation density of the thin film was  $5 \times 10^{11} \text{ line/m}^2$ .

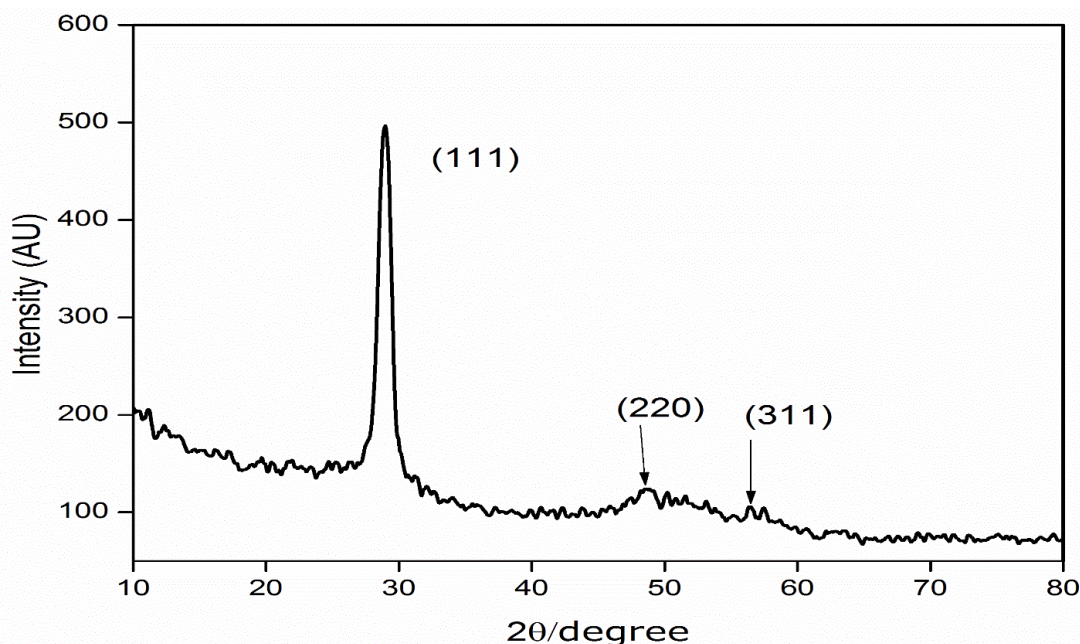


**Figure 1 :** XRD patterns of ZnS Thin films.

**Table 1:** Experimental d spacing and lattice parameter a value compared with data card (04-004-3804) for ZnS:

Plane (h k l)	Size (nm)	Experimental d value ( $\text{\AA}$ )	Lattice Parameter a ( $\text{\AA}$ )	Standard d value ( $\text{\AA}$ )	Card Lattice parameter ( $\text{\AA}$ )
(111)	10	3.109	5.369	3.1236	5.4102
(220)	8.7	1.868	5.283	1.9128	
(311)	39.3	1.640	5.439	1.612	

**Optical analysis of thin film:**

The optical transmission and reflection spectra of ZnS thin film in the wavelengths range from 200 to 2500 nm are shown in Fig. (2). It is clear from Fig.(2) that all transmittance spectrum show interference fringes in all range of wavelength with a sharp fall at the band edge in the range of 300-400 nm; whereas the interference effects disappear below this range. The intensity value of the interference fringe is around 90% in the transparent region. This value was found to be gradually decreasing when the wavelength approaches the absorption edge region.

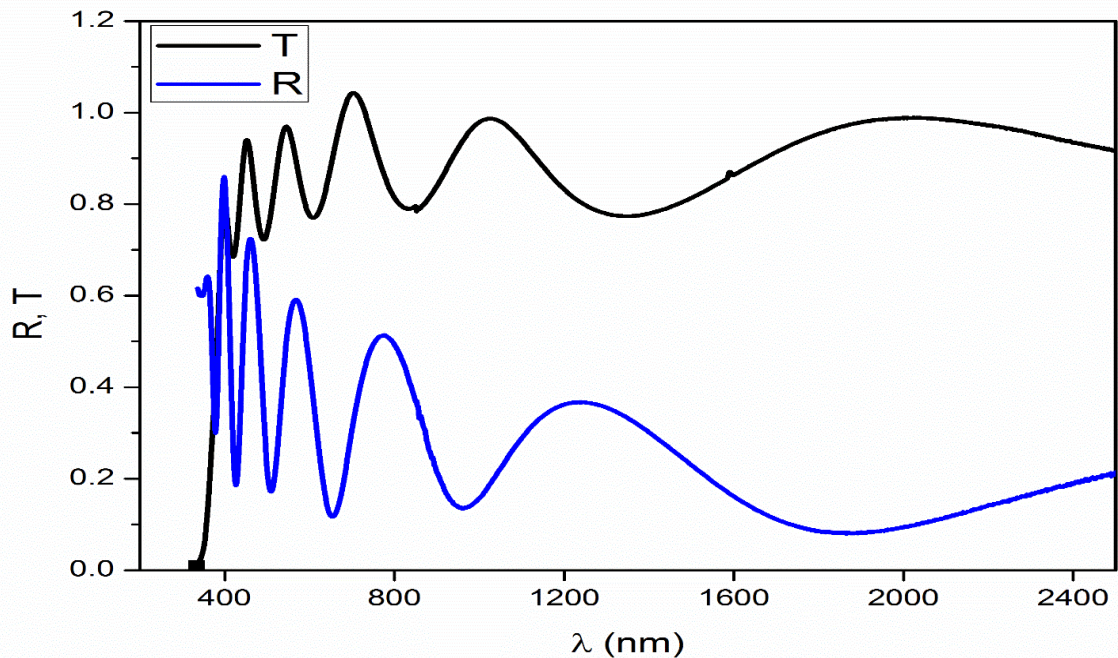


**Figure 2** the spectral distribution of transmittance and reflectance of as-deposited ZnS film.

The absorption coefficient  $\alpha(h\nu)$  was calculated from the experimental values of transmittance  $T(\lambda)$  and reflectance  $R(\lambda)$  by using equation (3) [15].

The optical band gaps ( $E_g$ ) of ZnS film was evaluated from the optical transmittance and reflectance data using the Tauc's relation equation (4)[16, 17]

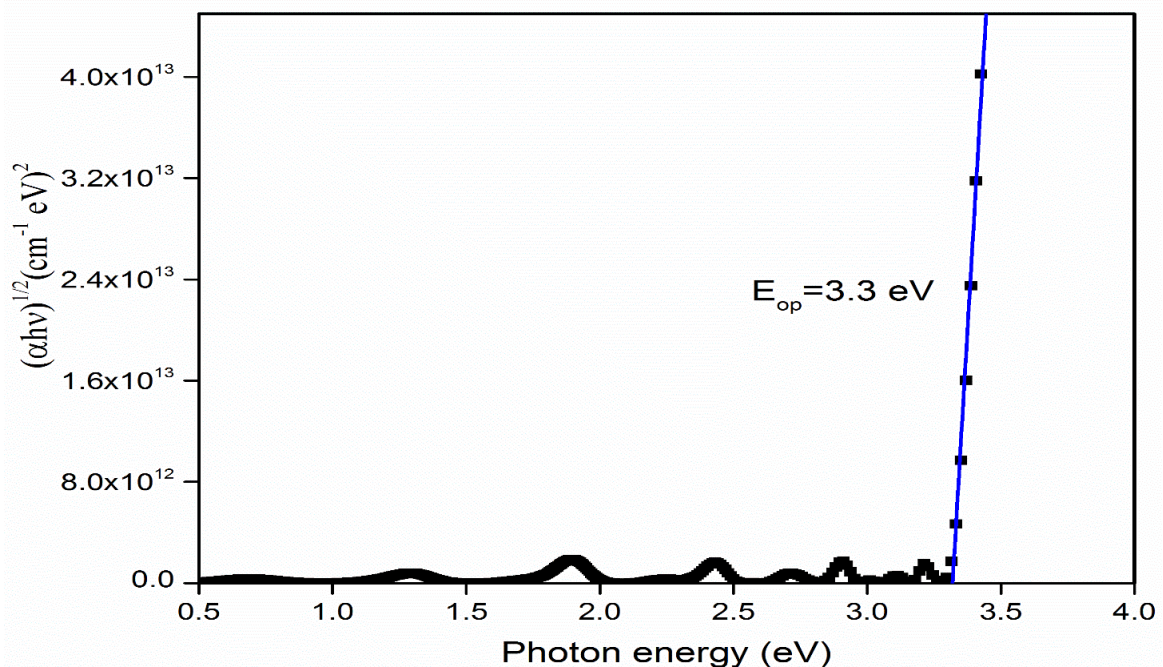


**Fig.(3)**Direct optical band gap of ZnS film deposited on quartz substrate.

The value of the optical band gap is calculated by extra-plotting the linear part of  $(\alpha h\nu)^{1/2}$  vs.  $h\nu$  graph in the strong absorption region as shown in fig.(3). The obtained band gap value of the sample is 3.3 eV[18, 19]. Such value seems to be consistent with the previously reported values [4, 20]

**Evaluation of the refractive index and absorption coefficient:**

The extinction coefficient,  $k$ , and the refractive index,  $n$ , of ZnS material thin film are pivotal parameters to determine the optical parameters and play a vital effect for the optoelectronic applications and device fabrication. They were estimated utilizing the following relations [21]:

$$k = \frac{\alpha\lambda}{4\pi} \quad (5)$$

$$n = \left( \frac{1+R}{1-R} \right) + \sqrt{\frac{4R}{(1-R)^2} - k^2} \quad (6)$$

The dispersion curve of refractive index,  $n$ , and the extinction coefficient,  $k$ , versus photon energy in the range from 0.5 eV to 3.5 eV, is shown in Fig.4. It demonstrates that the anomalous dispersion in the energy range  $h\nu \leq 3$  eV exists at all peaks, which be a function in refraction fringes.

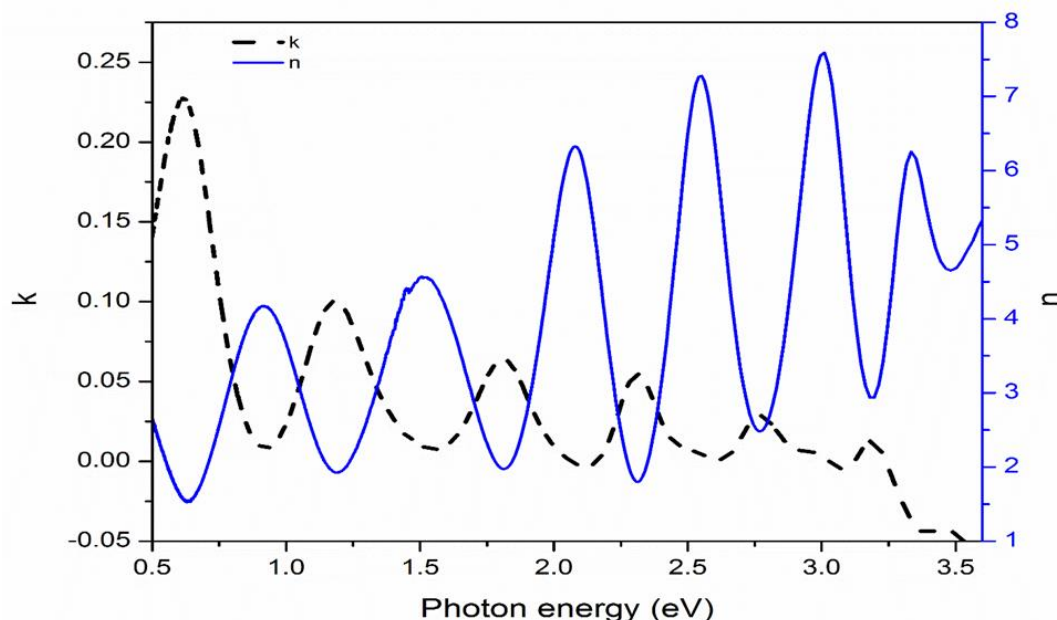


**Figure 4** The spectral distribution of the refractive index and extinction coefficient for ZnS thin films.

**Photoluminescence analysis:**

The photoluminescence, PL, spectra of ZnS thin films shown in fig.(5). The PL spectra of the ZnS thin film is recorded at room temperature for the excitation wavelengths 340 nm.

The emission spectrum shows a maximum at 340 nm and the asymmetric curve implies superposition of multiple emission bands. With 340 nm excitation, the PL spectra show an intense peak at 399 nm and two weak peaks at 435 nm 525 nm beside peak at 640 nm for the film. The violet-blue emission at 399, 430 and 468 nm may be ascribed to a transition involving vacancy states of ZnS films [22]. The luminescence peak around 399 nm is associated with the zinc vacancies [23] while the emission at 435 nm may be ascribed to S vacancies [24]. The peak centered at (486 nm) is due to the recombination between CB to a trap states emission of ZnS ( $V_{zn}$ ) [25]. The 525 nm emission has been attributed to elemental sulfur species on the surface of the sample [26]. The orange emission at 585 nm may be due to the nanoparticles [27, 28]. The 640 nm emission may be due to the lattice defect [29].

In different material of semiconductors, the luminescence can occur due to excitonic and trapped emissions. The inter impurity may induce effects on the intensity luminescence peaks observed in the spectrum of the measured film. Besides, most of peaks occur at an energy lower than the optical band gap indicating the presence of impurity states in the mid band gap region. This type of luminescence is due to emissions associated with the vacancy states [30].

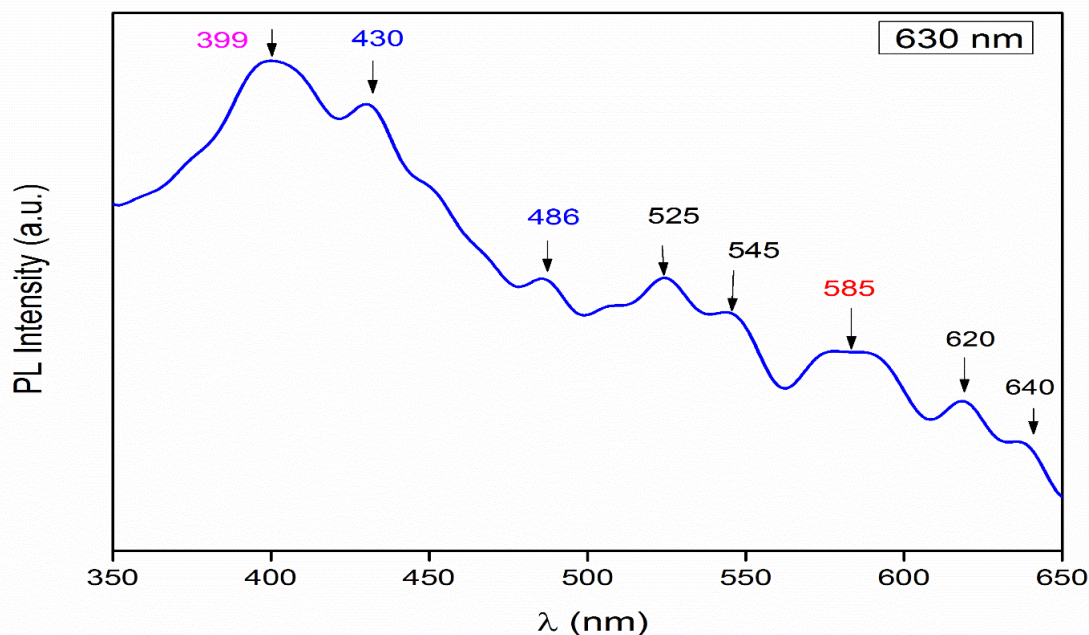


**Figure 5** Photoluminescence (PL) emission spectra of ZnS films.

#### IV. Conclusions:

Thin film of ZnS of nanocrystallite size has been successfully produced from ZnS nanocrystals synthesized by co-precipitation technique. The XRD pattern of ZnS exhibits the main strong reflection peak at  $d$  value =  $3.1 \text{ \AA}$ . Such peak corresponds to the (111) plane. Two other reflection peaks with weak intensity were observed and referred to planes (220) and (331) at  $d = 1.868 \text{ \AA}$  and  $1.640 \text{ \AA}$  respectively. Such peaks confirm the formation of ZnS in a cubic zinc blend structure with a lattice constant  $\sim 5.3460 \text{ \AA}$ . The average crystallite size is about  $19.3 \text{ nm}$ . The optical properties of ZnS thin film were manifested through T and R measurements. Direct allowed optical transitions with energy gap of about  $3.3 \text{ eV}$ . Maximum emission was observed at  $399 \text{ nm}$  was attributed to Zn vacancies while the emission noticed at  $435 \text{ nm}$  was attributed to the S vacancies.

#### References:

- [1]. H. Kim, W. Sigmund, *Journal of crystal growth*, 255 (2003) 114-118.
- [2]. B. Barman, K. Sarma, *Chalcogenide Lett*, 8 (2011) 171-176.
- [3]. B. Barman, P.K. Mochahari, K.C. Sarma, *AIP Conference Proceedings*, American Institute of Physics, 2011, pp. 116-118.
- [4]. J.P. Borah, J. Barman, K. Sarma, *Chalcogenide Lett*, 5 (2008) 201-208.
- [5]. J. Barton, P. Ranby, *Journal of Physics E: Scientific Instruments*, 10 (1977) 437.
- [6]. N. Dalacu, A. Kitai, *Applied physics letters*, 58 (1991) 613-615.
- [7]. J.H. Lee, Sooho Choi, Dayeon Jang, Du-Jeon, *Nanoscale*, 10 (2018) 14254-14263.
- [8]. X.X. Wang, Zhong Huang, Hongtao Liu, Zhe Chen, Di Shen, Guozhen, *Journal of Materials Chemistry*, 22 (2012) 6845-6850.
- [9]. S. Sahu, K. Nanda, *PROCEEDINGS-INDIAN NATIONAL SCIENCE ACADEMY PART A*, 67 (2001) 103-130.
- [10]. C.A. Guasch, N Kamoun Jebbari, N Turki, N Kamoun, *Journal of Alloys and Compounds*, 501 (2010) 85-88.
- [11]. R. Vishwakarma, *Journal of Theoretical and Applied Physics*, 9 (2015) 185-192.
- [12]. V. Ramasamy, K. Praba, G. Murugadoss, *Superlattices and Microstructures*, 51 (2012) 699-714.
- [13]. A. Ubale, D. Kulkarni, *Bulletin of Materials Science*, 28 (2005) 43-47.
- [14]. C. Pathak, D. Mishra, V. Agarwala, M. Mandal, *Materials science in semiconductor processing*, 16 (2013) 525-529.
- [15]. I. Zedan, A. Azab, E. El-Menyawy, *Spectrochimica Acta Part A: Molecular and Biomolecular Spectroscopy*, 154 (2016) 171-176.
- [16]. S. Mohamed, N. Hadia, M. Hasaneen, M.A. Hassan, *Materials Science in Semiconductor Processing*, 72 (2017) 72-77.
- [17]. N. Hadia, M. Hasaneen, M.A. Hassan, S. Mohamed, *Journal of Materials Science: Materials in Electronics*, 29 (2018) 4155-4162.
- [18]. D.H. Hwang, J.H. Ahn, K.N. Hui, K. San Hui, Y.G. Son, *Nanoscale research letters*, 7 (2012) 1-7.
- [19]. M.P. Sarma, G. Wary, *American Journal of Materials Science and Technology*, 4 (2015) 58-71.
- [20]. H.R. Dizaji, A.J. Zavaraki, M. Ehsani, *Chalcogenide Letters*, 8 (2011) 231-237.
- [21]. S. Wemple, *Physical Review B*, 7 (1973) 3767-3777.
- [22]. G.S. Arandhara, P.K Bora, *Journal of Basic and Applied Engineering Research*, 2 (2015) 1761-1764.
- [23]. H.-Y. Lu, S.-Y. Chu, S.-S. Tan, *Journal of Crystal growth*, 269 (2004) 385-391.
- [24]. D. Denzler, M. Olschewski, K. Sattler, *Journal of applied physics*, 84 (1998) 2841-2845.
- [25]. J. Hasanzadeh, *Acta Phys. Pol. A*, 129 (2016) 1147-1150.
- [26]. C. Ye, X. Fang, G. Li, L. Zhang, *Applied Physics Letters*, 85 (2004) 3035-3037.

- [27]. R.G. Bhargava, D Hong, X Nurmikko, A, Physical Review Letters, 72 (1994) 416-426.
- [28]. J.K. Salem, T.M. Hammad, S. Kuhn, I. Nahal, M.A. Draaz, N.K. Hejazy, R. Hempelmann, Journal of Materials Science: Materials in Electronics, 25 (2014) 5188-5194.
- [29]. S.R. Chalana, R. Vinod Kumar, A.P. Detty, I. Navas, K.S. Sreedevi, V.P. Mahadeva, IEEE Xplore, (2009) 1-6.
- [30]. X. Zhang, H. Song, L. Yu, T. Wang, X. Ren, X. Kong, Y. Xie, X. Wang, Journal of luminescence, 118 (2006) 251-256.